Downloaded from http://rsif.royalsocietypublishing.org/ on January 24, 2017

JOURNAL OF THE ROYAL SOCIETY Interface

CrossMark click for updates

J. R. Soc. Interface (2012) **9**, 2120–2130
doi:10.1098/rsif.2012.0121
Published online 2 May 2012

Assessing the impact of marine wind farms on birds through movement modelling

Elizabeth A. Masden[1,*], Richard Reeve[1], Mark Desholm[3], Anthony D. Fox[3], Robert W. Furness[2] and Daniel T. Haydon[1]

[1]*Boyd Orr Centre for Population and Ecosystem Health, Institute of Biodiversity, Animal Health and Comparative Medicine, College of Medical, Veterinary and Life Sciences, and* [2]*College of Medical, Veterinary and Life Sciences, University of Glasgow, Glasgow G12 8QQ, UK*
[3]*Department of Bioscience, Aarhus University, Kalø, Grenåvej 14, DK-8410 Rønde, Denmark*

Advances in technology and engineering, along with European Union renewable energy targets, have stimulated a rapid growth of the wind power sector. Wind farms contribute to carbon emission reductions, but there is a need to ensure that these structures do not adversely impact the populations that interact with them, particularly birds. We developed movement models based on observed avoidance responses of common eider *Somateria mollissima* to wind farms to predict, and identify potential measures to reduce, impacts. Flight trajectory data that were collected post-construction of the Danish Nysted offshore wind farm were used to parameterize competing models of bird movements around turbines. The model most closely fitting the observed data incorporated individual variation in the minimum distance at which birds responded to the turbines. We show how such models can contribute to the spatial planning of wind farms by assessing their extent, turbine spacing and configurations on the probability of birds passing between the turbines. Avian movement models can make new contributions to environmental assessments of wind farm developments, and provide insights into how to reduce impacts that can be identified at the planning stage.

Keywords: environmental impact assessment; barriers to movement; collision; common eider; *Somateria mollissima*; Nysted offshore wind farm

1. INTRODUCTION

Many countries are increasing their use of renewable energy (in particular, wind energy) in an effort to curb the effects of climate change. Increasing numbers of wind farms are being developed both onshore and offshore, with potentially negative effects on wildlife, especially birds. When birds exhibit avoidance behaviour towards turbines, wind farms may act as barriers to movement [1,2], increasing flight distances and so elevating energy expenditure. A lack of avoidance behaviour puts birds at risk from mortality through collision with these structures [3,4]. Wind farms may also affect birds through habitat loss, either directly as a consequence of the turbine 'footprints' or indirectly through avian avoidance responses to turbines [5–7].

The ability to predict how individual birds respond to a range of different wind turbine locations and configurations would be beneficial during wind farm planning to minimize barrier effects and/or collision risk. For example, under what circumstances are birds more likely to fly around or through an array of turbines? Until recently, the only types of movement data available on bird and wind farm interactions were: (i) observational watches recorded during environmental impact assessments (EIAs) consisting mainly of information on flying heights in the immediate vicinity of the wind farm; or (ii) long-distance movements from bird ring recoveries that provide general information on movements, from which it may be deduced, assuming the most direct route, whether a bird could have interacted with a wind farm. Therefore, it was not possible until recently to describe in detail the movements of birds in response to wind turbines; however, technologies such as surveillance radar and satellite/GPS telemetry can now provide accurate movement data at finer spatial and temporal resolutions [8–11].

Despite being an important factor in determining animal distributions, animal movement often remains poorly understood [12,13]. Advances in the accuracy, energy management and miniaturization of animal location tags are now providing a rich source of data, which can be used to quantitatively study movement paths [12,14–19]. Methods to quantify animal movement can be mapped onto a continuum, ranging from those that describe emergent or summary properties

*Author and address for correspondence: Environmental Research Institute, Centre for Energy and the Environment, North Highland College UHI, University of the Highlands and Islands, Thurso, Caithness KW14 7EE, UK (elizabeth.masden@thurso.uhi.ac.uk).

Electronic supplementary material is available at http://dx.doi.org/10.1098/rsif.2012.0121 or via http://rsif.royalsocietypublishing.org.

Received 14 February 2012
Accepted 16 February 2012

This journal is © 2012 The Royal Society

Downloaded from http://rsif.royalsocietypublishing.org/ on January 24, 2017

of the data such as sinuosity, first passage time, scale invariance and fractal dimension [20–22], to explicitly mechanistic models that aim to describe the underlying movement process. These more complex 'parametric' models can be used to identify dependencies between animal movement and biotic or abiotic features co-occurring on the landscape [14,17], often using modified correlated random walks or diffusion processes [23,24]. The increase in cheap and accessible computing power enables relatively complex parameter-rich models to be fitted to data using Bayesian model-fitting machinery. The same model formulations can then be used to link movement processes to features of the landscape or covariates such as habitat type, and then to predict an animal's movement path, allowing one to anticipate the consequences of landscape change. Because our goal was to study the effects of wind farm design on bird avoidance behaviour, we adopt this second approach in what follows.

The aim of this study was to illustrate how data collected during the EIA process could be used to aid planning and development of future wind farms, and minimize their impacts on wildlife. This study is, to our knowledge, the first of its kind to apply current methods from movement ecology to radar data collected during the post-construction assessment of an offshore wind farm, and to quantitatively describe the movements of birds around a wind farm. Fitting complex models to data is often limited by classical estimation techniques; therefore, we used Bayesian methods of analysis and performed inference with Just Another Gibbs Sampler (JAGS, [25]). We give two examples of how such a model can be used to improve the assessment of the impacts of wind farms on birds: (i) the effect of wind farm dimensions on the number of birds passing between turbines; and (ii) the effect of different configurations of turbines on the avian permeability of a wind farm.

2. METHODS

2.1. Data collection and processing

Data were collected from the Nysted offshore wind farm, which comprises 72 wind turbines in eight north–south-oriented rows, 850 m apart at 480 m intervals east–west, covering an area of *ca* 60 km^2 in the western Baltic Sea south of Denmark. Flight trajectories of flocks of autumn-migrating common eider *Somateria mollissima* were recorded during the daytime using surveillance radar mounted on an observation tower *ca* 5 km from the wind farm [26]. For the duration of observation periods, all turbines were operational; therefore, observations are of eider flocks mainly responding to active turbines. An estimated 345 000 common eiders migrate past the Nysted offshore wind farm every year, from breeding areas in the northern Baltic to wintering areas in the Inner Danish waters and in the Wadden Sea [26]. Flocks of birds entering the detection area created an echo on the radar monitor, and by observing the echoes, the migration trajectories of these flocks could be determined (see Desholm & Kahlert [1] for data collection methods). Only east–west trajectories were used in this study owing to the position of the radar station in relation to the wind farm and the predominant orientation of autumn migration. Of these trajectories, we used only those that came within 500 m of a wind turbine, as birds showed very little response to the wind farm at distances greater than this [2]. The selected trajectories were converted from continuous lines to discrete points at 100 m intervals using ArcGIS (v. 9.3) and Hawth's Analysis Tools for GIS [27]. On the basis of the relative linearity and the length of the movement trajectories, sampling steps of 100 m were judged to be a sensible use of computer time while resulting in no loss of movement information. The trajectories were sampled at regular distance intervals rather than at time intervals because flight speeds of migrating eider are remarkably constant [28]. The final dataset contained 89 flock trajectories each comprising 70–230 data points (median = 127). Flight trajectory data were collected for 24 days, between 11 September 2003 and 28 October 2005, and the flock sizes associated with these trajectories ranged from 7 to 200 individuals (median = 35).

2.2. Models

Here we present four models, each designed to describe the movements of birds in response to wind turbines. Models 1 and 2 assume that all birds respond in the same way, i.e. the parameters are constant across all individuals, while models 3 and 4 are hierarchical and include individual variation, i.e. hyper-parameters are sampled for each individual from a population level distribution. We assume that individual birds travel directly, and at a constant speed [28] from a starting location towards a final destination, and exhibit avoidance behaviour towards wind turbines. The turbines are assumed to rotate at a constant speed because of the gearing mechanism associated with the generator. For each observation, j, along a particular trajectory i (obs_{ij}), the models estimate the direction of movement to the next observation (obs_{ij+1}) by resolving the forces attracting a bird to its final destination and repelling it away from a wind farm, the proportion of each depending on the distance between the bird and the wind farm (see figure 1 for a diagram), and the method of resolution differing between models. The direction ($\boldsymbol{\Phi}$, measured in radians) between each pair of observations is assumed to be independently drawn from a wrapped Cauchy distribution with parameters $\boldsymbol{\mu}$ (the mean direction) and $\boldsymbol{\rho}$ (the mean cosine of the angular distribution). The wrapped Cauchy is one of a number of possible circular distributions available, and exploratory analyses revealed the wrapped Cauchy distribution to better fit the data than the von Mises distribution. The likelihood function for the data modelled this way is

$$L(\boldsymbol{\phi}_{11} \cdots \boldsymbol{\phi}_{Nn_N} | \boldsymbol{\mu}_{11} \cdots \boldsymbol{\mu}_{Nn_N}, \boldsymbol{\rho}) = \prod_{i=1}^{N} \prod_{j=1}^{n_i-1} C(\boldsymbol{\phi}_{ij}, \boldsymbol{\mu}_{ij}, \boldsymbol{\rho}), \tag{2.1}$$

where N is the number of trajectories (i.e. 89) n_i is the total number of observations in trajectory i, $\boldsymbol{\phi}_{ij}$ is the observed direction of the next point in the trajectory

Downloaded from http://rsif.royalsocietypublishing.org/ on January 24, 2017

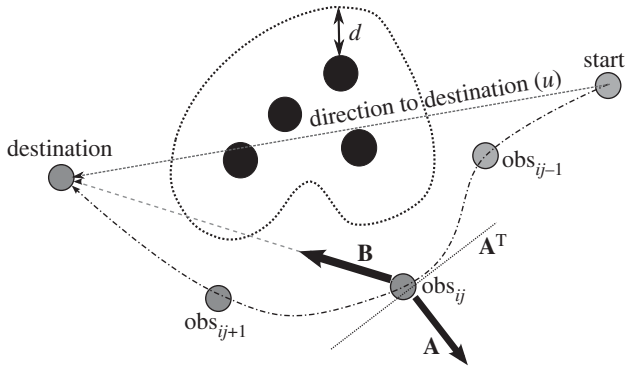

Figure 1. A diagram of the general principles of the model with an example movement trajectory (dot-dashed line) and variables within the model. Black filled circles represent wind turbines, while grey filled circles represent the positions of birds along the trajectory. $\mathbf{A}$ is the overall repulsion exerted on a bird at a given location by the wind farm; $\mathbf{A}^{\mathbf{T}}$ is the perpendicular vector to $\mathbf{A}$; $\mathbf{B}$ is the vector of attraction towards the final destination and d is the distance at which a bird turns halfway from $\mathbf{B}$ to $\mathbf{A}^{\mathbf{T}}$.

from point j, μ_{ij} is the predicted mean direction and C denotes the wrapped Cauchy distribution [29] with density function

$$C(\phi, \mu, \rho) = \frac{1}{2\pi}\frac{1-\rho^2}{1+\rho^2 - 2\rho\cos(\phi-\mu)} \qquad (2.2)$$
$$0 \le \mu < 2\pi,\ 0 \le \rho \le 1,\ 0 \le \phi < 2\pi.$$

(i) *Model 1*

A model that assumes the direction of travel is simply the sum of the attractive force and the repellent force of the turbines (adjusted by a scaling factor). The repelling force, $\mathbf{V}_{ijk}$, exerted by each turbine in the wind farm is described with an inverse power law with power p, thus

$$\mathbf{V}_{ijk} = \frac{1}{l_{ijk}^p}\mathbf{e}_{ijk}, \qquad (2.3)$$

where $\mathbf{e}_{ijk}$ is the unit vector from the kth wind turbine in the direction of the jth observed location of trajectory i, and l_{ijk} is the distance between these two points. $\mathbf{A}_{ij}$, which can be split into its x and y components (a_x/a_y), is the sum of these forces summed over all turbines and is the overall repulsion exerted on a bird at a given location by the wind farm and is therefore given by

$$\mathbf{A}_{ij} = \sum_k \mathbf{V}_{ijk}. \qquad (2.4)$$

The attraction towards the final destination is represented by the vector $\mathbf{B}$, where u is the bearing/direction to the final destination. The distance between the starting location (obs$_{i1}$) and the final destination (obs$_{in_i}$) is assumed to be sufficiently great that $\mathbf{B}$ does not change substantively over the course of the trajectory, thus

$$\mathbf{B} = \begin{pmatrix} \cos u \\ \sin u \end{pmatrix}. \qquad (2.5)$$

The resultant unit vector ($\mathbf{F}_{ij}$) describing the direction of travel is thus

$$\begin{pmatrix} \cos\mu_{ij} \\ \sin\mu_{ij} \end{pmatrix} = \frac{\mathbf{B} + c\mathbf{A}_{ij}}{|\mathbf{B} + c\mathbf{A}_{ij}|}, \qquad (2.6)$$

where c is a scaling factor and from which we can derive the bearing μ_{ij}. The bird then travels in this direction.

(ii) *Model 2*

A model constrained to contour round the turbines. Vectors $\mathbf{A}_{ij}$ and $\mathbf{B}$ are again the overall repulsion of the wind farm and attraction of the destination respectively, and are estimated as for model 1 but $\mathbf{F}_{ij}$, the resultant direction of travel, is no longer a simple weighted sum of the two. Instead we choose a direction between that of the bird's destination and a contour of equal repulsion around the wind farm. This ensures that the bird moves away from the wind farm towards its destination, tending to move closer to its destination at nearly all times, while contouring round the wind farm as necessary. We calculate one direction of the contour $\mathbf{A}'_{ij}$, perpendicular to $\mathbf{A}_{ij}$, and then choose which direction to travel on the contour, $\mathbf{A}^{\mathbf{T}}_{ij}$, with a probability dependent on which direction is closer to that of its destination (inverse logit is a sigmoidal function that maps the real numbers onto [0,1]). We then set the resultant direction of travel, $\mathbf{F}_{ij}$, to be a weighted sum of $\mathbf{A}^{\mathbf{T}}_{ij}$ and $\mathbf{B}$, scaled by the extent to which $\mathbf{A}_{ij}$ and $\mathbf{B}$ are in the same direction:

$$\begin{aligned} b_{ij} &= \mathrm{logit}^{-1} k_{\mathrm{b}}\left(\mathbf{A}_{ij}\cdot\mathbf{B} + \frac{1}{d^p}\right), \\ \mathbf{F}'_{ij} &= b_{ij}\mathbf{B} + (1-b_{ij})\frac{\mathbf{A}^{\mathbf{T}}_{ij}}{|\mathbf{A}^{\mathbf{T}}_{ij}|}, \\ \mathbf{F}_{ij} &= \frac{\mathbf{F}'_{ij}}{|\mathbf{F}'_{ij}|}, \end{aligned} \qquad (2.7)$$

where

$$\mathbf{A}' = \begin{pmatrix} -a_y \\ a_x \end{pmatrix} \quad \text{and}$$

$$\mathbf{A}^{\mathbf{T}} = \begin{cases} \mathbf{A}' & \text{with probability } \mathrm{logit}^{-1} k_c \mathbf{A}'\cdot\mathbf{B} \\ -\mathbf{A}' & \text{otherwise} \end{cases}$$

At each movement step, a bird must choose whether to fly directly towards its destination ($\mathbf{B}$) or to follow the contour ($\mathbf{A}^{\mathbf{T}}_{ij}$) in response to the turbines. The direction of travel will be close to $\mathbf{B}$ when $\mathbf{A}_{ij}$ is sufficiently small or when travelling in the direction of $\mathbf{B}$ decreases the wind farm repulsion ($\mathbf{A}_{ij}\cdot\mathbf{B}$ is positive). Consequently, b_{ij} will be close to 1 and the bird will continue directly to its final destination. However, b_{ij} will be closer to 0 and the bird will turn more towards $\mathbf{A}^{\mathbf{T}}_{ij}$ when $\mathbf{A}_{ij}$ is large, and travelling in the direction of $\mathbf{B}$ increases repulsion ($\mathbf{A}_{ij}\cdot\mathbf{B}$ must be negative). In the absence of strong repulsion, the bird will follow $\mathbf{B}$.

The decision on how far to turn towards $\mathbf{A}^{\mathbf{T}}_{ij}$ depends on the distance to the turbines: the parameter d is the distance from a single turbine at which a bird would

Downloaded from http://rsif.royalsocietypublishing.org/ on January 24, 2017

Table 1. Prior distributions for the parameters in the models.

parameter	description	prior
u	bearing to final destination	uniform (3.1, 3.6)
$\boldsymbol{\rho}$	the cosine of the angular distribution of the wrapped Cauchy	uniform (0.7, 1)
c	model 1 scaling factor	uniform (0, 100)
d	distance at which bird turns halfway from $\mathbf{B}$ to $\mathbf{A}_{ij}^{\mathbf{T}}$	uniform (0.2, 5)
p	power of repelling kernel	uniform (1, 5)
k_{b}	how quickly bird moves from $\mathbf{B}$ to $\mathbf{A}_{ij}^{\mathbf{T}}$	uniform (0, 20)
k_{c}	how frequently the bird will turn in the correct direction	uniform (−20, 0)
shape	shape parameter of gamma distribution of individual d_{i} values	gamma (0.01, 0.01)
$\boldsymbol{\tau}$	precision of normal distribution of u_{i} values	uniform (1, 100)

turn exactly half-way from $\mathbf{B}$ to $\mathbf{A}_{ij}^{\mathbf{T}}$, and k_{b} is a scaling factor that determines how quickly the bird's direction shifts from $\mathbf{B}$ to $\mathbf{A}_{ij}^{\mathbf{T}}$ as its distance to the turbines decreases. For example, a high value of k_{b} will make a bird turn away suddenly at d, whereas a low value will make it start turning away at a small angle earlier. However, in either case, when the bird has approached sufficiently close to the turbines, it will follow the $\mathbf{A}_{ij}^{\mathbf{T}}$ contour, which keeps the magnitude of the repulsion constant until it can get round them.

As well as deciding how much to turn away, the bird must also choose which direction to turn. If $\mathbf{A}_{ij}$ and $\mathbf{B}$ are in exactly opposite directions, then the bird will randomly choose either left or right, as neither choice will make it reach its destination quicker. Otherwise, the bird will tend to turn from $\mathbf{B}$ in the direction in which $\mathbf{A}_{ij}$ is closer, which should correspond to the shorter route round the turbines. Whether the bird is to turn to the right or to the left is determined by a Bernoulli random variable. The scaling factor k_{c} determines how frequently the bird will turn in the correct direction, with high absolute values of k_{c} indicating that it will always choose the shorter route to its destination while a zero value for k_{c} would indicate a 50 : 50 chance of going either way around the wind turbine array.

(iii) *Model 3*

In model 2, we assumed that parameters were constant across all trajectories. In model 3, we relaxed this assumption and fitted the hyper-parameter d_{i} separately for each of the 89 trajectories to include individual variation in the distance at which birds responded to the wind turbines. The d_{i} values were taken from a gamma distribution because d_{i} must be positive and the gamma distribution takes only real and positive values:

$$d_{\mathrm{i}} \sim \mathrm{gamma}\left(\mathrm{shape}, \frac{\mathrm{shape}}{d}\right). \tag{2.8}$$

(iv) *Model 4*

In model 3, we fitted the hyper-parameter d_{i} separately for all trajectories but assumed that u was constant across all trajectories. In model 4, in addition to fitting d_{i} separately, we also fitted the hyper-parameter u_{i} separately for each of the 89 trajectories to include individual variation in the bearing to the final destination. The u_{i} values were taken from a normal distribution because it was known that all birds were heading in approximately the same direction, but that there would be some variation around this mean direction. However, the variation was unlikely to span 2π and 0, meaning a circular distribution was not required:

$$u_{\mathrm{i}} \sim \mathrm{normal}\ (\bar{u}, \sigma^2). \tag{2.9}$$

2.3. Model parameterization

Models were fitted using Monte Carlo Markov chain (MCMC) techniques as implemented in JAGS [25]. Priors were all diffuse and uninformative (for prior distributions, see table 1). For each model, we ran three MCMC chains for 100 000 iterations and examined convergence and autocorrelation for the model parameters. Convergence was assessed using the Gelman–Rubin convergence statistic [30], which compares variance between and within Markov chains. Values close to 1 indicate convergence.

2.4. Goodness of fit

To compare the fit of the four competing models, we used posterior predictive checks (PPCs) [31]. We used the PPC method rather than a deviance information criterion [32] because it allowed us to assess the ability of models to fit properties of the movement trajectories not explicitly included in the modelling process [14]. Choosing unmodelled features of the trajectories guards against rewarding overfitting to the data, and we further avoid this by randomizing the individual flock parameters (where present) and their simulated starting positions. We assessed whether movement trajectories produced by the models had features similar to those observed in the data for three characteristics: (i) the number of trajectories that entered the middle of wind farm, i.e. trajectories that passed between the five central turbines on the eastern boundary of the wind farm. This feature of the data was chosen because it quantified the number of individuals entering and moving through the central area of the wind farm and not only the periphery; (ii) the number of trajectories that passed to the south versus the north of the wind farm and did not enter the array; and (iii) the straightness index of trajectories. The straightness index (which indicates deviation from a straight line) is the ratio of the net movement divided by the gross movement and is described in Benhamou [21]. Data more than 5 km east of the eastern edge of the wind farm were excluded from the PPC calculations of the straightness index because we were

Downloaded from http://rsif.royalsocietypublishing.org/ on January 24, 2017

interested in movements in response to the wind turbines. Five kilometres were considered large enough to include any potential long-range avoidance responses.

We sampled from the joint posterior distribution of each model to obtain matched combinations of parameters, sampling equally from each of the 89 tracks when the model contained trajectory-specific parameters. The final size of the posterior chain, and thus the number of independent parameter combinations present, was used to determine the number of parameter sets that could be extracted. Movement trajectories were then simulated using these sampled parameters, with starting locations selected from the original data. This simulation process was repeated 50 times for each parameter set to account for the stochasticity in the model, and the characteristics of trajectories were recorded and compared against the original data. The model that produces tracks that were most representative of the original data was chosen for the remainder of the study.

2.5. Simulations

Using the parameter estimates from the best chosen candidate model, we simulated movement trajectories of birds through areas with wind turbines. We ran simulations to investigate:

(i) the effect of wind farm dimensions, i.e. inter-turbine distances and the number of turbines, on the number of birds passing between turbines, and
(ii) the effect of different configurations of turbines on the avian permeability of a wind farm.

(i) *The effect of wind farm dimensions on the number of birds passing between turbines*
If a species has a high risk of collision mortality, it is beneficial to design wind farms that ensure the birds do not fly through the array of wind turbines. Therefore, it is important to be able to predict the number of birds likely to pass between turbines at varying turbine spacing. A wind farm comprises horizontal rows of turbines and vertical columns. Ignoring potential constraints on turbine spacing owing to the effects on turbine efficiency, we varied the distance between rows of turbines (from 200 to 1000 m at intervals of 20 m) and also the number of columns in an array (from 1 to 8), using the Nysted wind turbine array as a template. We simulated 100 trajectories for each combination of inter-turbine distance and number of columns, and recorded the number of trajectories that entered the wind farm through the central five turbines on the eastern boundary of the wind farm. To account for any possible differences owing to approach angle, the trajectories were started from 10 different locations.

(ii) *The effect of different configurations of turbines on the avian permeability of a wind farm*
Some species may be more sensitive to increased energy costs due to wind farms acting as barriers to movement, rather than having a high risk of collision mortality. In these situations, it may be more important to have permeability through a wind farm development area. We define avian permeability as the capacity of a delimited development area to be infiltrated by birds. Avian permeability was assessed by computing a straightness index as described in Benhamou [21]. If an area was completely permeable, then the distance measures would be the same and the straightness index would be one. The greater the disparity, the less permeable the area and smaller the index of straightness. We investigated the permeability of a 100 km^2 area containing 100 turbines in different configurations. This average turbine density (1 turbine km^{-1}) is similar to that of the Nysted wind farm (1.2 turbines km^{-1}) yet still allowed plausible scenarios to be explored. The concept of a specific area within which turbines could be placed was intended to represent, albeit at a smaller scale, development areas such as the Crown Estate's round three zones or exclusivity agreement areas and constrain turbines to within a defined area. The scenarios were:

(i) equal spacing across the 100 km^2 development area (inter-row distance = 1000 m; inter-column distance = 1000 m);
(ii) diamond configuration with equal spacing across the development area;
(iii) equal spacing within the central 25 km^2 (inter-row distance = 500 m; inter-column distance = 500 m);
(iv) four blocks containing 25 turbines with equal spacing (inter-row distance = 500 m; inter-column distance = 500 m); and
(v) random spacing with the 100 km^2 development area.

For each scenario, we simulated 100 trajectories using our best fitting model. To account for any possible differences owing to approach angle, this was repeated from 10 different start locations on an arc 20 km from the centre of the 100 km^2 area, giving a total of 1000 simulated trajectories. Twenty kilometres was considered a suitable distance, as this corresponded to the maximum distances from the centre of the Nysted wind farm to start points of the observed data used to parameterize the model. The trajectories were targeted through the centre of the 100 km^2 area; therefore, in the absence of the wind farm, all trajectories would cross at the centre point.

3. RESULTS

3.1. Parameters

We generated 600 000 samples from the posterior distributions of all parameters using three chains, a burn-in period of 100 000, and an initial thinning rate of 1 in 100. For all parameters, chains were considered to have converged with Gelman–Rubin convergence statistic values less than 1.2; however, autocorrelation was detected between posterior samples of the parameters d and p. We therefore thinned these samples further by a rate of 1 in 6 to give a final sample size of 500.

A summary of parameter estimates is presented in table 2 and density and trace plots for the parameters are included in the electronic supplementary material.

Downloaded from http://rsif.royalsocietypublishing.org/ on January 24, 2017

Table 2. Mean estimates of parameters within the models (lower and upper bounds of 95% credible intervals). (M-dash (—) indicates where parameters were not included in models.)

parameter	model 1	model 2	model 3	model 4
u	3.246 (3.240, 3.252)	3.291 (3.285, 3.296)	3.296 (3.292, 3.300)	3.291 (3.269, 3.312)
ρ	0.855 (0.852, 0.859)	0.884 (0.881, 0.887)	0.899 (0.896, 0.901)	0.920 (0.918, 0.923)
c	0.013 (0.011, 0.015)	—	—	—
d	—	0.266 (0.253, 0.278)	0.239 (0.221, 0.256)	0.244 (0.228, 0.260)
p	0.482 (0.372, 0.608)	1.701 (1.651, 1.743)	1.599 (1.558, 1.639)	1.621 (1.579, 1.664)
k_b	—	0.319 (0.306, 0.332)	0.387 (0.374, 0.400)	0.380 (0.369, 0.392)
k_c	—	−1.350 (−1.524, −1.177)	−1.323 (−1.499, −1.155)	−0.803 (−0.883, −0.727)
shape	—	—	25.24 (18.08, 33.75)	25.22 (18.07, 34.11)
τ	—	—	—	81.11 (58.36, 97.63)

Model 1 estimated u to be 3.24 radians, and models 2–4 produced estimates of 3.29 radians, putting the destination point in a south-westerly direction. Model 1 was distinctly different from the other models that shared parameters with similar estimates and overlapping credible intervals. For example, the mean estimate of d was 0.266 (95% CI = 0.253, 0.278) for model 2, 0.239 (95% CI = 0.221, 0.256) for model 3 and 0.244 (95% CI = 0.228, 0.260) for model 4, therefore, models 3 and 4 described trajectories that responded to turbines only when they were closer compared with model 2. The mean estimate for k_b was also less for model 2 than for models 3 and 4 therefore models 3 and 4, described trajectories that responded more suddenly at distance d to the turbines rather than turning away earlier. Parameter p was greater for model 2 than for models 1, 3 and 4; therefore the repelling kernel extended further from the turbines for model 2 while model 1 had the least repulsion ($p = 0.48$). The shape parameter in models 3 and 4 was estimated at 25.24 (95% CI = 18.08, 33.75) and 25.22 (95% CI = 18.07, 34.11), respectively. In model 4, $\tau(\sigma^{-2})$ was estimated to be 81.11. Therefore, the individual d_i hyper-parameters were distributed with a mean of d and a standard deviation of 0.05, while the individual u_i hyper-parameters were distributed with a mean of u and a standard deviation of 0.01.

3.2. Model selection

To assess the fit of models, we compared features of the original data to simulated tracks using PPCs. The characteristics compared were: (i) number of tracks entering the central area of the wind farm, (ii) number of tracks flying south versus north of the wind farm (assessed as the number of tracks flying south divided by the number flying north), and (iii) the straightness index. For each characteristic compared as a PPC, there were 22 250, i.e. 50 replicates of 445, simulated tracks. Five of the original data tracks (5.62%) entered the central area of the wind farm. The mean percentage of simulated tracks entering the wind farm was 42.20 per cent (95 percentile interval = 38.65%, 45.84%) for model 1, 0 per cent for model 2, 5.49 per cent (95 percentile interval = 4.30%, 6.74%) for model 3 and 4.23 per cent (95 percentile interval = 3.15%, 5.40%) for model 4. Of the original 89 tracks, 52 (58.43%) flew to the south of the wind farm, while 9 (10.11%) flew around the north, giving a ratio of 5.78 to 1. For model 1, the mean percentage of flights travelling south versus north of the wind farm was 20.21 (95 percentile interval = 10.20%, 38.02%), for model 2 = 38.89% (95 percentile interval = 22.88%, 63.53%), model 3 = 44.60% (95 percentile interval = 24.07%, 82.26%) and for model 4 = 4.40% (95 percentile interval = 3.86%, 5.12%). The mean straightness index of the original data was 0.917 (95 percentile interval = 0.799, 0.978) while for model 1 the index was 0.982 (95 percentile interval = 0.981, 0.982), for model 2 was 0.940 (95 percentile interval = 0.937, 0.943), for model 3 was 0.947 (95 percentile interval = 0.944, 0.949) and for model 4 was 0.937 (95 percentile interval = 0.934, 0.940). Models 3 and 4, i.e. those that included individual variation, had characteristics most similar to the observed data and of these, model 4 was more representative across the three PPCs (figure 2). Model 4 was therefore adopted as the best fitting model and used to simulate tracks for the remainder of the study.

3.3. Simulations

(i) *The effect of wind farm dimensions on the number of birds passing between turbines*

As the distance between turbines increased, so did the proportion of birds travelling between turbines (figure 3). With eight columns of turbines at 200 m spacing, no birds passed between the turbines. Increasing the inter-turbine distance to 500 m increased the percentage of birds to more than 20 per cent, while a spacing of 1000 m increased this further to 99 per cent. For a given distance between turbine rows, increasing the number of columns in a wind farm decreased the number of birds entering the array. A distance of 500 m between turbine rows caused 99 per cent of birds to enter the wind farm when there was only one column of turbines, while increasing the size of the wind farm to two columns decreased this to 83 per cent. Therefore, by increasing the number of turbine columns in an array, it was possible to increase the inter-turbine distance and raise the threshold before which 50 per cent of birds entered the wind farm (figure 3).

(ii) *The effect of different configurations of turbines on the avian permeability of an area*

The permeability, i.e. straightness index of the area differed for each of the turbine scenarios (figure 4). The straightness index ranged from 0.796 to 0.998 across

Downloaded from http://rsif.royalsocietypublishing.org/ on January 24, 2017

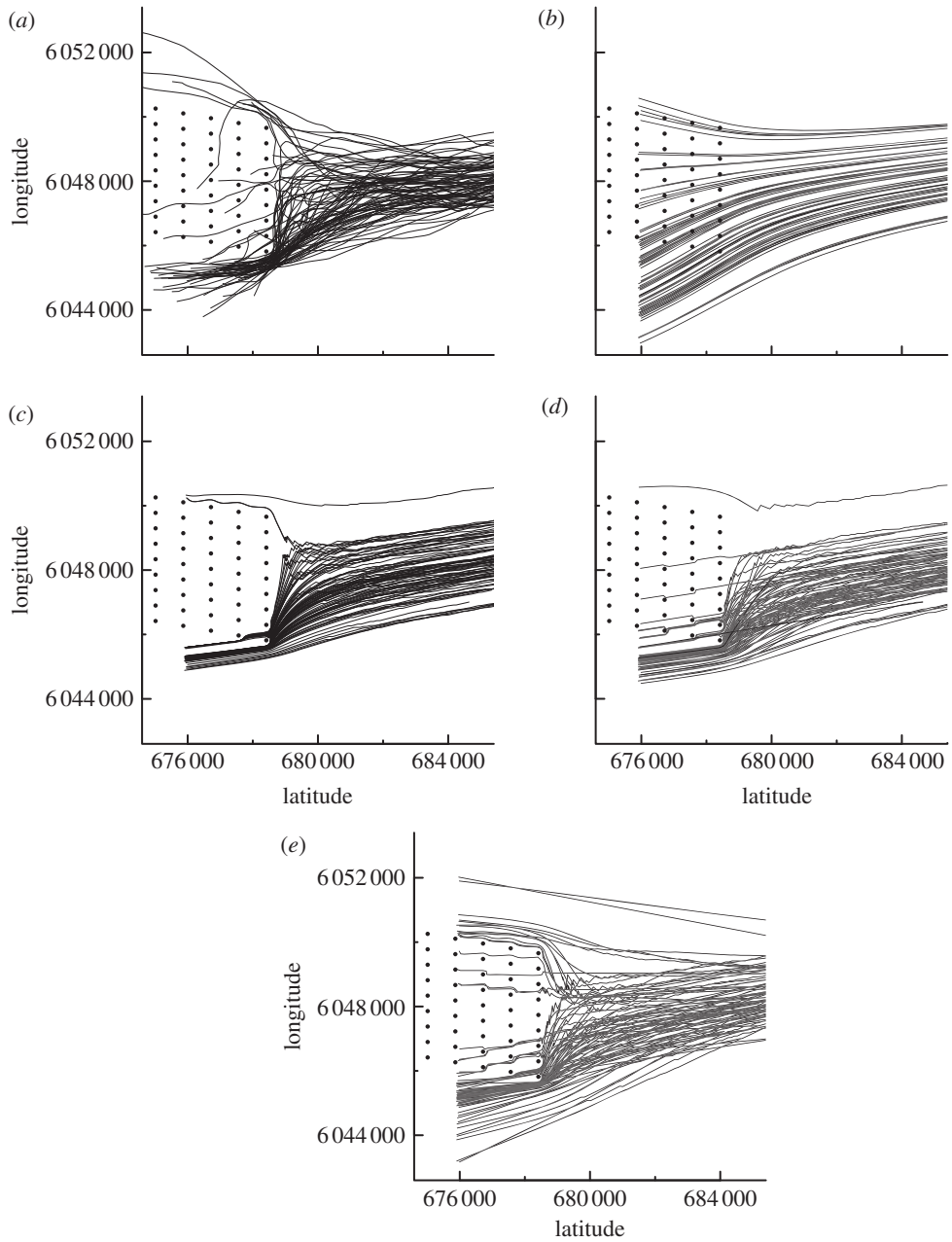

Figure 2. Example movement trajectories of common eider around the Nysted offshore wind farm, Denmark: (*a*) 89 observed tracks, and 89 tracks simulated using parameters from (*b*) model 1, (*c*) model 2, (*d*) model 3 and (*e*) model 4. Black dots denote wind turbines. Note that apparent thick lines are due to superimposition of trajectories. Data are projected using the Universal Transverse Mercator (UTM) geographic coordinate system (zone 32° N). Latitude and longitude are displayed in metres.

the scenarios. Scenario (iv) (four blocks of turbines) had the highest mean straightness index and was therefore highly permeable (mean = 0.989, range = 0.868–0.998) while scenario (iii) (central block of turbines) had the lowest mean straightness index (mean = 0.952, range = 0.843–0.998). However, scenario (ii) (diamond configuration) had the single lowest value for straightness at 0.796.

4. DISCUSSION

We demonstrate how data collected on bird movements, post-construction of a wind farm can be used to parametrize avian movement models. This has practical applications in EIAs of wind farm developments and associated implications for planning. Such models are increasingly important, because the European Union has set targets to generate 20 per cent of its energy from renewable sources by 2020 [33] and hence there has been a rapid increase in numbers of proposed wind farm developments. With more wind farms, concerns grow over the potential adverse effects of their cumulative impacts on wildlife populations, in particular birds. Despite increasing numbers of avian studies on the effects of wind farms, there remains a lack of understanding of the interactions, i.e. avian avoidance response, between birds and wind turbines for many species, limiting the ability to predict the likely effects of future developments.

Wind farm EIAs and post-construction monitoring invariably record bird movement data in and around

Downloaded from http://rsif.royalsocietypublishing.org/ on January 24, 2017

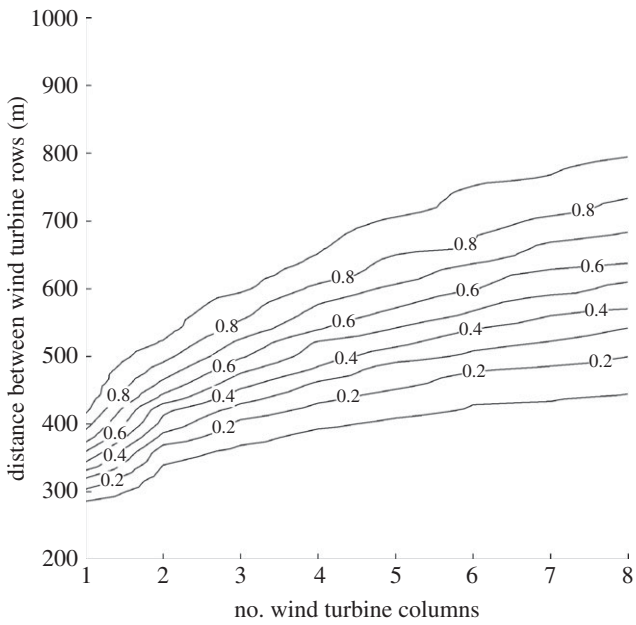

Figure 3. Contour plot of the proportion of simulated eider trajectories entering a wind farm through the central five turbines on the eastern boundary. Wind farms comprised varying numbers of columns, and distances between the turbine rows varied.

the (proposed) wind farm development area. The types of data recorded range from visual observations, i.e. vantage point watches [34] to radar and telemetry data [1,8] with the latter becoming increasingly available. The increase in data associated with individual birds gathered at finer resolution presents an opportunity to investigate the (potential) impacts of wind farms on birds using techniques not previously used in this research field. To date, the majority of data analyses regarding avian movements around wind farms have been qualitative, e.g. describing species-specific flight heights and abundance, although some studies have taken a more quantitative approach using statistical models for example, to assess golden eagles *Aquila chrysaetos* home ranges and space use [35]. One obvious exception is the Band model [36], which is a mechanistic model to estimate collision risk. In this study, we present a method using mechanistic models parameterized using radar data, data increasingly recorded at wind farm sites, in an effort to bridge this quantitative analytical gap.

Of the movement models presented, model 4 captured more of the variability in the observed data with simulated trajectories more closely resembling observed trajectories (figure 2). Model 4 incorporated the most individual variation with variation in both the distance at which birds responded to the wind turbines and the bearing to the final destination, suggesting that individual behaviour is a significant factor that should be considered when formulating these movement models. As well as graphically exploring the data, we assessed model fit using PPCs ((i) the number of simulated trajectories to enter the wind farm through the central five turbines on the eastern boundary of the wind farm, i.e. the middle of the wind farm; (ii) the number of tracks that navigated to the south versus the north of the wind farm; and (iii) the straightness index). Even though these features of the data were not modelled explicitly, they were adequately captured by model 4, indicating this to be the preferred model. A modification that could improve model fit would be to model turning angle between movement steps as well as bearing, as this would incorporate any autocorrelation between the movement steps.

In this study, we provide two example uses of a model to support the environmental assessment process of wind farms. The first example is relevant for species vulnerable to collision and thus applicable to known species' hot spots, e.g. migration corridors or wintering/breeding areas. For such species, it is beneficial to be able to predict the dimensions and spatial configuration of turbines that would reduce the probability that individuals fly through the wind farm. By varying turbine row spacing, and column number, we influenced the number of birds entering the centre of the wind farm (figure 3); the smaller the spacing, the fewer birds entered the wind farm. Also, as the number of rows in an array increased, the greater the inter-turbine distance could be before birds flew between turbines. Both these results hold owing to the avoidance response of the birds. However, birds continued to pass between peripheral turbines, for example cutting off a corner rather than flying straight through the entire array, suggesting that designs eliminating corners may be beneficial. Of the configurations presented in this study, it was the diamond array (figure 4*b*,*g*) oriented with the main direction of travel, i.e. east to west, which produced the lowest straightness index record. The availability of such ecological knowledge enables wind farm design to balance technological and engineering constraints (for example, the minimum and optimal proximity of turbines and their placement [37]) with environmental considerations.

For species known to avoid wind farms, turbines ultimately act as barriers to movements with the consequent additional distance travelled increasing normal energy requirements. This may especially be the case for breeding seabirds, which forage several times a day and may commute past wind farms [38]. To explore the concept of permeability, we considered five different wind farm scenarios (figure 4), and simulated trajectories of birds travelling through the developed area. Permeability was least when turbines were spaced equally across the central 25 km^2 area (scenario (iii)), causing individuals to travel further to reach their destination (figure 4*c*,*h*). Although scenario (ii) (diamond configuration) had the lowest single value of straightness index, it was a function of the orientation of the diamond configuration and overall scenario (iii) would keep more birds from passing between turbines, thus reducing collision risk, while having the least impact in terms of energetic requirement. The diamond configuration (scenario (ii)) proved less permeable than a square of similar size (scenario (i)) when oriented in line with the main direction of movement (figure 4*a*,*b*,*f*,*g*) with more birds directed around the outside of the turbine array. This suggests that a diamond array may reduce the number of birds entering

Downloaded from http://rsif.royalsocietypublishing.org/ on January 24, 2017

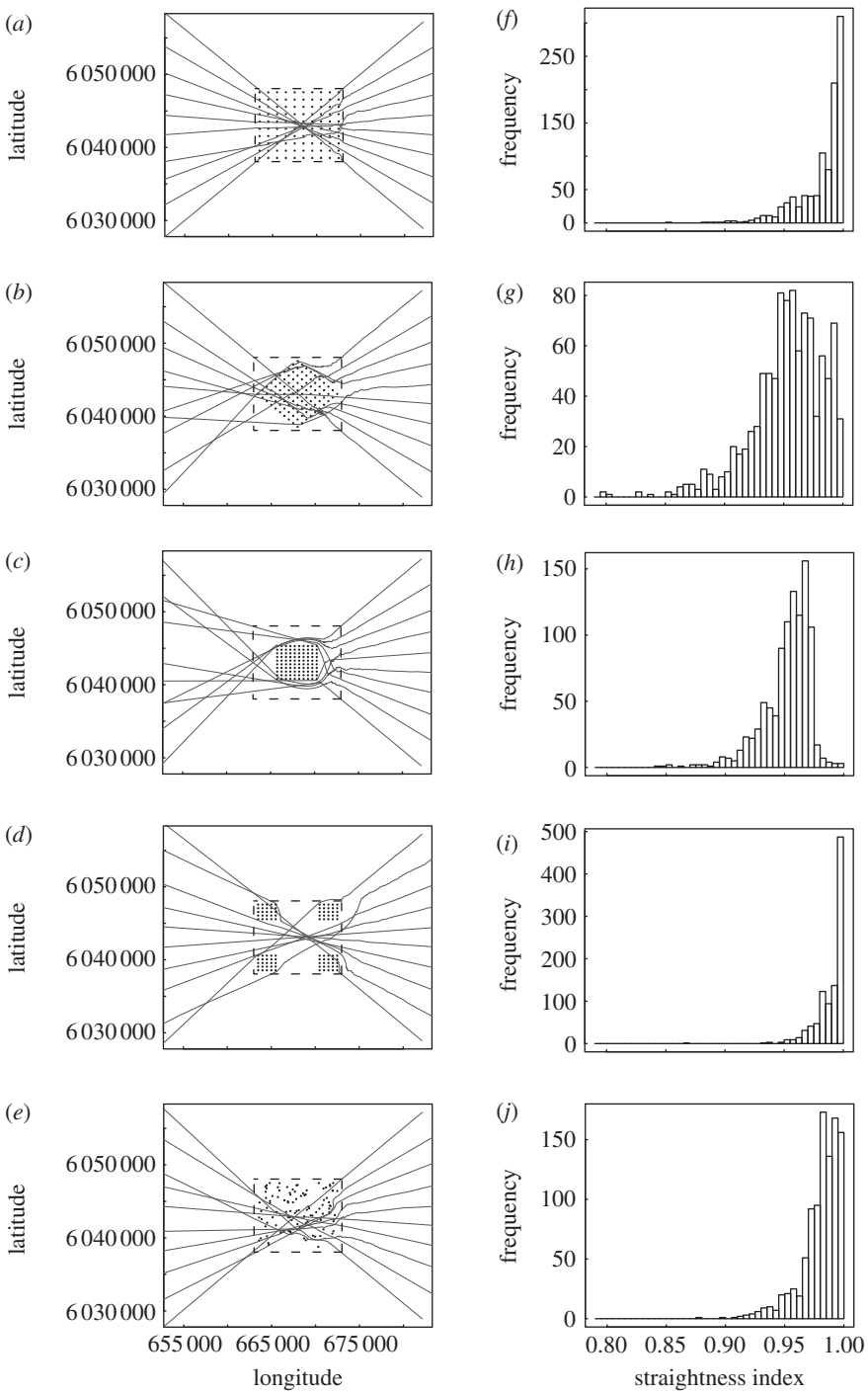

Figure 4. Permeability results for different wind farm scenarios. (*a*–*e*) Plots of example eider trajectories. Grey lines represent simulated trajectories. Black dots represent wind turbines. Dashed box represents the 100 km^2 wind farm area. (*f*–*j*) Histograms of straightness index assuming wind farm scenarios (i)–(v) ((i) equal spacing across the 100 km^2 development area. Inter-row distance = 1000 m and inter-column distance = 1000 m; (ii) diamond configuration with equal spacing across the development area; (iii) equal spacing within the central 25 km^2. Inter-row distance = 500 m and inter-column distance = 500 m; (iv) four blocks containing 25 turbines with equal spacing. Inter-row distance = 500 m and inter-column distance = 500 m; and (v) random spacing with the 100 km^2 development area). Data are projected using the UTM geographic coordinate system (zone 32° N). Latitude and longitude are displayed in metres.

a wind farm and thus being at risk from collision. Four blocks of turbines (scenario (iv)) had the greatest permeability and the least variation, suggesting for this example at least, that having several smaller wind farms may have advantages over one larger wind farm when barriers to movement is the main concern. Such a modelling approach provides extensive opportunities to explore scenarios and the potential impacts on bird movements, thus incorporating environmental considerations in the optimal wind farm design.

The results generated by this study are based on several assumptions. We assume that avian avoidance behaviour is manifest at the level of the wind turbine, and although cumulative, the repulsion is not to the

Downloaded from http://rsif.royalsocietypublishing.org/ on January 24, 2017

wind farm structure as a single entity. This is an assumption of the model and consequently the model predicts that a bird is more likely to avoid an array of wind turbines than to avoid a single row of turbines and this is perhaps unlikely for all species. The model was parametrized using data collected from a single species, common eider, and it is unlikely that all species exhibit the same behaviour. However, this is, to our knowledge, the first attempt at such a model and with more data for different species, the model could be extended. Also, owing to limitations of the data collection method, the model was parameterized only with data from the daytime and it would benefit from additional night-time data as birds may respond differently. The model presented describes only changes in movement in terms of latitude and longitude because the data available were from surveillance radar, but it is known that birds may also adjust their altitude in response to a wind farm, although apparently not affecting the avoidance response [1]. Similarly, we model movements around a wind farm surrounded by sea; so topography will have no influence on bird movements, yet this would not be the case for onshore wind farms where birds are likely to respond to a variable landscape. Wind speed was also excluded from the model because the avoidance response has previously been shown to be consistent irrespective of the entire range of experienced crosswind conditions [1,25]. Eider migration generally takes place under good conditions (eiders stop migrating during inclement weather, such as very strong winds and in the face of frontal systems and heavy precipitation); so the results presented are expected to be representative of normal migratory conditions.

In conclusion, we demonstrate that avian movement models enhance wind farm planning and enable a more flexible approach that can incorporate not only economic and engineering, but also ecological data to reduce the negative effects of wind farms on birds. In the future, our ability to parameterize such models depends entirely on data availability. There is a lack of post-construction monitoring and associated data [4,39] and it is fundamental that this shortfall is rectified to further progress.

Many thanks to Hawthorne Beyer and Matthew Denwood for advice on Bayesian methods. Also thanks to Louise Matthews and three anonymous reviewers for comments on previous versions of this manuscript. Data were collected as part of the Danish Demonstration Project running at the Nysted offshore wind farm, funded by the Danish Public Service Obligation funds (PSO funds) that are financed by a small fraction of each consumer's electricity bill, and allocated to research and development projects. E.A.M. was funded by a postgraduate studentship from Scottish Natural Heritage. R.R. was funded by the European Commission's Seventh Framework Programme (FP7/2007-2013) under grant agreement no. 226556 (FMD-DISCONVAC).

REFERENCES

1 Desholm, M. & Kahlert, J. 2005 Avian collision risk at an offshore wind farm. *Biol. Lett.* **1**, 296–298. (doi:10.1098/rsbl.2005.0336)

2 Masden, E. A., Haydon, D. T., Fox, A. D., Furness, R. W., Bullman, R. & Desholm, M. 2009 Barriers to movement: impacts of wind farms on migrating birds. *ICES J. Mar. Sci.* **66**, 746–753. (doi:10.1093/icesjms/fsp031)

3 Erickson, W. P., Johnson, G. D. & Young Jr, D. P. 2005 A summary and comparison of bird mortality from anthropogenic causes with an emphasis on collisions. In *Proc. 3rd Int. Partners in flight Conf., 20–24 March 2002, Asilomar, CA*. US Forest Service General Technical Report PSW-191 (eds C. J. Ralph & T. D. Rich), pp. 1029–1042. Albany, CA: US Dept. of Agriculture, Forest Service, Pacific Southwest Research Station.

4 Langston, R. H. W., Fox, A. D. & Drewitt, A. L. 2006 Conference plenary discussion, conclusions and recommendations. *Ibis* **148**, 210–216. (doi:10.1111/j.1474-919X.2006.00512.x)

5 West, A. D. & Caldow, R. W. D. 2006 The development and use of individuals-based models to predict the effects of habitat loss and disturbance on waders and wildfowl. *Ibis* **148**, 158–168. (doi:10.1111/j.1474-919X.2006.00520.x)

6 Pearce-Higgins, J. W., Stephen, L., Langston, R. H. W. & Bright, J. A. 2008 Assessing the cumulative impacts of wind farms on peatland birds: a case study of golden plover *Pluvialis apricaria* in Scotland. *Mires Peat* **4**, 1–13.

7 Madders, M. & Whitfield, D. P. 2006 Upland raptors and the assessment of wind farm impacts. *Ibis* **148**, 43–56. (doi:10.1111/j.1474-919X.2006.00506.x)

8 Bevanger, K. *et al.* 2008 Pre- and post-construction studies of conflicts between birds and wind turbines in coastal Norway. Progress report 2008, no. 409, Norwegian Institute for Nature Research, Trondheim, Norway.

9 Gauthreaux, S. A. & Belser, C. G. 2003 Radar ornithology and biological conservation. *Auk* **120**, 266–277. (doi:10.1642/0004-8038(2003)120[0266:ROABC]2.0.CO;2)

10 Kelly, T. A., West, T. E. & Davenport, J. K. 2009 Challenges and solutions of remote sensing at offshore wind energy developments. *Mar. Pollut. Bull.* **58**, 1599–1604. (doi:10.1016/j.marpolbul.2009.09.002)

11 Griffin, L., Rees, E. & Hughes, B. 2010 The migration of whooper swans in relation to offshore wind farms, WWT Final Report to COWRIE Ltd, WWT, Slimbridge.

12 Turchin, P. 1998 *Quantitative analysis of movement: Measuring and modelling population redistribution in animals and plants*. Sunderland, MA: Sinauer.

13 Nathan, R., Getz, W. M., Revilla, E., Holyoak, M., Kadmon, R., Saltz, D. & Smouse, P. E. 2008 A movement ecology paradigm for unifying organismal movement research. *Proc. Natl Acad. Sci. USA* **105**, 19 052–19 059. (doi:10.1073/pnas.0800375105)

14 Morales, J. M., Haydon, D. T., Frair, J., Holsiner, K. E. & Fryxell, J. M. 2004 Extracting more out of relocation data: building movement models as mixtures of random walks. *Ecology* **85**, 2436–2445. (doi:10.1890/03-0269)

15 Patterson, T. A., Thomas, L., Wilcox, C., Ovaskainen, O. & Matthiopoulos, J. 2008 State-space models of individual animal movement. *Trends Ecol. Evol.* **23**, 87–94. (doi:10.1016/j.tree.2007.10.009)

16 Viswanathan, G. M., Afanasyev, V., Buldyrev, S. V., Murphy, E. J., Prince, P. A. & Stanley, H. E. 1996 Levy flight search patterns of wandering albatrosses. *Nature* **381**, 413–415. (doi:10.1038/381413a0)

17 Smouse, P. E., Focardi, S., Moorcroft, P. R., Kie, J. G., Forester, J. D. & Morales, J. M. 2010 Stochastic modelling of animal movement. *Phil. Trans. R. Soc. B* **365**, 2201–2211. (doi:10.1098/rstb.2010.0078)

18 Hebblewhite, M. & Haydon, D. T. 2010 Distinguishing technology from biology: a critical review of the use of

Downloaded from http://rsif.royalsocietypublishing.org/ on January 24, 2017

GPS telemetry data in ecology. *Phil. Trans. R. Soc. B* **365**, 2303–2312. (doi:10.1098/rstb.2010.0087)

19 Cagnacci, F., Boitani, L., Powell, R. A. & Boyce, M. S. 2010 Animal ecology meets GPS-based radiotelemetry: a perfect storm of opportunities and challenges. *Phil. Trans. R. Soc. B* **365**, 2157–2162. (doi:10.1098/rstb.2010.0107)

20 Bailey, H. & Thompson, P. 2006 Quantitative analysis of bottlenose dolphin movement patterns and their relationship with foraging. *J. Anim. Ecol.* **75**, 456–465. (doi:10.1111/j.1365-2656.2006.01066.x)

21 Benhamou, S. 2004 How to reliably estimate the tortuosity of an animal's path: straightness, sinuosity, or fractal dimension. *J. Theor. Biol.* **229**, 209–220. (doi:10.1016/j.jtbi.2004.03.016)

22 Schick, R. S. *et al.* 2008 Understanding movement data and movement processes: current and emerging directions. *Ecol. Lett.* **11**, 1338–1350. (doi:10.1111/j.1461-0248.2008.01249.x)

23 Codling, E. A., Plank, M. J. & Benhamou, S. 2008 Random walk models in biology. *J. R. Soc. Interface* **5**, 813–834. (doi:10.1098/rsif.2008.0014)

24 Benhamou, S. 2006 Detecting an orientation component in animal paths when the preferred direction is individual-dependent. *Ecology* **87**, 518–528. (doi:10.1890/05-0495)

25 Plummer, M. 2009 JAGS: a program for analysis of Bayesian graphical models using Gibbs Sampling. In *Proc. 3rd Int. Workshop on Distributed Statistical Computing* (*DSC 2003*), *20–22 March*. Vienna, Austria.

26 Petersen, I. K., Christensen, T. K., Kahlert, J., Desholm, M. & Fox, A. D. 2006 *Final results of bird studies at the offshore wind farms at Nysted and Horns Reef*. Rønde, Denmark: NERI.

27 Beyer, H. L. 2004 Hawth's analysis tools for ArcGIS. See http://www.spatialecology.com/htools.

28 Desholm, M. 2003 How much do small-scale changes in flight direction increase overall migration distance. *J. Avian Biol.* **34**, 155–158. (doi:10.1034/j.1600-048X.2003.02974.x)

29 Fisher, N. I. 1993 *Statistical analysis of circular data*. Cambridge, UK: Cambridge University Press.

30 Gelman, A. & Rubin, D. B. 1992 Inference from iterative simulation using multiple sequences. *Stat. Sci.* **7**, 457–472. (doi:10.1214/ss/1177011136)

31 Gelman, A., Carlin, J. B., Stern, H. S. & Rubin, D. B. 2004 *Bayesian data analysis*. New York, NY: Chapman and Hall/CRC.

32 Spiegelhalter, D. J., Best, N. G., Carlin, B. P. & Van Der Linde, A. 2002 Bayesian measures of model complexity and fit. *J. R. Stat. Soc. B* **64**, 583–639. (doi:10.1111/1467-9868.00353)

33 House of Lords European Committee 2008 The EU's Target for Renewable Energy: 20% by 2020, 58 pp. HL Report 175-I. HMSO, London. http://www.publications.parliament.uk/pa/ld200708/ldselect/ldeucom/175/175.pdf (last accessed 28 April 2009).

34 Walker, D., McGrady, M., McCluskie, A., Madders, M. & McLeod, D. R. A. 2005 Resident golden eagle ranging behaviour before and after construction of a windfarm in Argyll. *Scott Birds* **25**, 24–40.

35 Fielding, A. H., Whitfield, D. P. & McLeod, D. R. A. 2006 Spatial association as an indicator of the potential for future interactions between wind energy developments and golden eagles *Aquila chrysaetos* in Scotland. *Biol. Conserv.* **131**, 359–369. (doi:10.1016/j.biocon.2006.02.011)

36 Band, W., Madders, M. & Whitfield, D. P. 2007 Developing field and analytical methods to assess avian collision risk at wind farms. In *Birds and wind farms* (eds M. De Lucas, G. F. E. Janss & M. Ferrer), pp. 259–275. Madrid, Spain: Quercus.

37 Crespo, A., Hernández, J. & Frandsen, S. 1999 Survey of modelling methods for wind turbine wakes and wind farms. *Wind Energy* **2**, 1–24. (doi:10.1002/(SICI)1099-1824(199901/03)2:1<1::AID-WE16>3.0.CO;2-7)

38 Masden, E. A., Haydon, D. T., Fox, A. D. & Furness, R. W. 2010 Barriers to movement: modelling energetic costs of avoiding marine wind farms amongst breeding seabirds. *Mar. Pollut. Bull.* **60**, 1085–1091. (doi:10.1016/j.marpolbul.2010.01.016)

39 Stewart, G. B., Pullin, A. S. & Coles, C. F. 2007 Poor evidence-base for assessment of windfarm impacts on birds. *Environ. Conserv.* **34**, 1–11. (doi:10.1017/S0376892907003554)